J. Biochem. 131, 427–435 (2002)

Second Derivative Fluorescence Spectra of Indole Compounds[1]

Suprabha Nayar,*,[2] Amrita Brahma,* Chaitali Mukherjee,† and Debasish Bhattacharyya*,[3]

Division of Protein Engineering, Indian Institute of Chemical Biology, 4, Raja S.C. Mallick Road, Jadavpur, Calcutta-700032, India; and †Department of Chemistry, University of Calcutta, 92, A.P.C. Road, Calcutta-700009, India

Received July 30, 2001; accepted December 26, 2001

The fluorescence emission spectrum of *N*-acetyl tryptophan amide (NATA) in 20 mM K-phosphate buffer, pH 7.5, with excitation at 295 nm, when subjected to second derivatization, showed two troughs at 340 ± 1.0 nm (A) and 358.5 ± 1.0 nm (B). Linear dependence of derivative intensities at A and B was observed with increasing NATA concentration between 0–30 nM but the intensity ratio (B/A), termed R, was found to be invariant at 0.70 ± 0.05. R remained unaffected with variation of the pH (4–10), temperature (15–70°C), salt concentration (0–2 M NaCl), and excitation wavelength between 280–300 nm. A 50-fold molar excess of *N*-acetyl tyrosine over 10 nM NATA and inclusion of a quencher like 0.8 M acrylamide, 0.4 M potassium iodide or trichloroethanol had no effect on R. It was, however, linearly dependent on the polarity of the solvent–in 1,4-dioxane it became 0.07 ± 0.05. Derivative spectra of tryptophans of proteins largely resembled that of NATA. Low R values of between 0.02–0.34 were observed for proteins under native conditions, which is consistent with the general buried character of tryptophan residues. R increased to 0.6–0.9 after unfolding with denaturants or extensive proteolysis and decreased to close to the original value after refolding. The equilibrium unfolding transitions of proteins expressed as R largely resembled the transitions measured using other physical parameters. R appears to be a more sensitive index for monitoring the hydrophobic environment of tryptophans in protein compared to parameters like emission maxima or intensity of underivatised spectra.

Key words: fluorescence spectra, NATA, protein conformation, second derivative, solvent polarity.

The resolution of a spectrum goes on increasing as it is derivatized against one of its parameters, usually the wavelength (*1*). The use of second derivative absorbtion spectroscopy for proteins in the ultra-violet region (260–320 nm) is well known. It has been used in the structural analysis of a number of proteins in terms of comparison of different mutants, ligand binding, unfolding, *etc.* (*2–6*, reviewed in Ref. *7*). In addition it has been used for the quantitation of tyrosine, tryptophan, and phenylalanine residues of proteins, as the absorption maxima of these residues are different (*8*). Fourth and higher derivative UV absorption spectroscopy was reviewed in Ref. *1*. In contrast, there has been a limited number of reports on derivatized fluorescence emission spectra. Neglecting the weak emission of phenylalanine, quantitative estimation of tyrosine and tryptophan residues of a protein can be performed by spectral derivatization (*9*). This procedure has been used to compare the fluorescence properties of human plasma lipo-proteins (*10*), and in the quantitation of some drugs and their metabolic products (*11–15*).

Here it has been investigated whether the derivatization of fluorescence emission can yield additional information over underivatized spectra about the environment of indole derivatives in solution or in a macromolecular structure like those of proteins, particularly during a change of conformation.

MATERIALS AND METHODS

Materials—*N*-Acetyl tryptophan amide (NATA, $\zeta_{280.8\ nm}$ = 5,690 M^{-1} cm^{-1}), *N*-acetyl tyrosine ($\zeta_{275.5\ nm}$ = 1,490 M^{-1} cm^{-1}) (*9*), tryptophan, 2-mercaptoethanol (2-MCE), SDS, standard proteins, and proteases were from Sigma, USA. Solvents (AR or GR) were purchased locally. Dehydrated ethyl alcohol was from Bengal Chemical and Pharmaceuticals, Calcutta. HPLC/spectral grade methanol, acetonitrile and sequential grade 8 M guanidine hydrochloride (Gdm, HCl) were from Pierce Urea (E. Merck, India) was recrystallized from hot ethanol.

Purity of NATA—The chemical homogeneity of the compound was verified by the appearance of a single spot on TLC on silica gel plates (2.5 × 8 cm) with three different solvents, isopropanol:water = 70:30; 95% ethanol:water = 70:30, and butanol:acetic acid:water = 80:20:20 after development in an iodine chamber. Homogeneity was further

[1] This research was assisted by Department of Science and Technology grants (SP/SO/D-45/93 and SP/SO/D-107/99) awarded to D.B. S.N. and A.B. were supported by a Research Associateship from the Council of Scientific and Industrial Research and the DST projects at different phases.

[2] Present address: National Metallurgical Laboratory, Jamshedpur-832007, Jharkhand, India.

[3] To whom correspondence should be addressed. Fax: +91-33-473-5197/0284, Phone: +91-33-473-3491 (ext. 164)

tested using a Waters μ-Bondapak C_{18} reverse phase HPLC column equilibrated with 0.1% trifluoroacetic acid (TFA) in water. After application of the sample, the equilibrating buffer was run for 20 min, followed by a linear water-methanol gradient containing 0.1% TFA set for 60 min at a flow rate of 0.5 ml/min. In the chromatogram, only one sharp and symmetrical peak was observed at the retention time of 48.5 min. The fluorophoric homogeneity of the compound was verified after altering the excitation wavelength between 280–300 nm and observing the normalised overlapping emission spectrum between 310–500 nm.

Purification of Proteins—UDP-galactose 4-epimerase (hereafter called epimerase) from *Escherichia coli* was purified after (*16*). The procured proteins (listed in Table II) were further purified by passage through a precalibrated Water's Protein Pak 300 size-exclusion (SE)-HPLC column equilibrated with 50 mM Na-phosphate buffer, pH 7.5, containing 0.1 M NaCl. Elution was followed at 280 nm. The major peak, which corresponded to the native molecular weight of the respective protein, was pooled and used directly. Protein concentrations were determined either from extinction coefficients (*17*) or after Lowry with BSA as a reference (*18*), where the concentration was too low or the spectral data were not available.

Second Derivative Fluorescence Spectrum—All fluorescence measurements were performed with a Hitachi F4020 spectrofluorimeter using a 700 μl square-headed quartz cuvette after excitation at 295 nm unless otherwise stated. For each recording, two spectra were scanned between 300–500 nm, where the sample in buffer and the buffer as a control were termed [X] and [Y]. Corrected emission spectra were generated after subtraction of the spectral data, [X]–[Y], using the arithmetic program of the in built software. This is an obligatory requirement because no matter how small the emission peaks of the control spectra are, they may induce significant error in the derivatized sample spectra. Derivatization of the corrected spectrum was performed using the derivative mode of the data processor. The derivative data scale was properly adjusted for spectral intensity measurements.

Changing of the excitation and emission band passes between 0.2–20 nm did not alter the spectral characters to any significant extent except the intensity. Therefore a band pass of 5 nm was maintained throughout. A delta derivative of 5 or 50 nm either yielded a spectrum too noisy to be interpreted or failed to resolve troughs in the negative ordinates–a delta derivative of 10 nm was found to be optimum. However, the "curve smooth" function applied to the corrected spectrum before or after derivatization did not appropriately improve the spectral quality.

Precision of Derivatization—A fluorescence emission spectrum having a single peak has the following characters: an emission maximum (em_{max}), point O, where the gradient of the curve is zero, and two points, A and B, on either sides of em_{max} having the maximum positive and negative gradients, respectively. On the first derivatization, points A and B appear as a peak and a trough, respectively, and point O will touch the abscissa. On the second derivatization, points A and B touch the abscissa, and point O appears in the negative ordinate, which is sometimes difficult to identify experimentally. Three samples, bovine serum albumin (BSA) and lysozyme in 20 mM K-phosphate buffer, pH 7.4, and lysozyme in the same buffer containing 4 M urea equilibrated for 16 h, were arbitrarily selected for spectral measurements (ex: 280 nm). Identification of points A, B, and O for the three samples are shown in Table I. It shows that the precision of measurements was within ± 4 nm. The inaccuracy originated mainly from the failure of the instrument to register the zero-ordinate of the derivative profile, which had stiff gradients at these points. It was also observed that in every case the derivatized value near the end of the emission zone, say at 500 nm, converged to ± 0.001.

Distinguishing the Raman Peak from Water—Excitation of an aqueous buffer at 295 nm gives rise to a small Raman contribution between 323–333 nm having a maximum at 328 nm. In cases where the quantum yield of tryptophan residues is weak, for example, in the case of some proteins, it is necessary to increase the sample concentration to increase the fluorescence intensity. Thus, once the optical density of the sample begins to increase, the Raman peak due to the sample is inherently less than that due to the solvent as a control–a phenomenon comparable to the inner filter effect (*19, 20*). In such a case subtraction of a solvent blank leads to over correction of the Raman peak. This phenomenon apparently did not affect the present study because the intensity of the Raman peak at 333 nm, a position 5.5 nm ahead of the first trough concerned in this study (338.5 nm), is essentially zero; the optical densities of the proteins used were around 0.1 at 295 nm and 0.001 at 320 nm onward making the inner filter effect insignificant, and finally the inner filter effect cannot change the emission pattern of a fluorophore, except the intensity, where the sample exhibits no absorption at the emission zone, and hence the derivative pattern too, except the intensity.

Unfolding, Refolding, and Extensive Proteolysis of Proteins—The proteins (0.5–2 mg/ml) were incubated with 0–8 M urea or 6 M Gdm, HCl in 20 mM Na-phosphate buffer, pH 7.5, for 16 h at 25°C to allow unfolding at equilibrium. In the case of reduction of cysteine bridges, samples were incubated with denaturants in the presence of 10 mM 2-MCE at 80°C for 4 h, followed by equilibration as stated. Refolding of proteins was initiated by 20–50-fold dilution with buffer, followed by standing 8 h for equilibration (*21, 22*). The native proteins were subjected to trypsin digestion (1:25, w/w) in 50 mM Tris, HCl buffer, pH 8.5, at 37°C with a booster dose added after 4 h, followed by overnight incubation with chymotrypsin (1:20, w/w). The degraded proteins were analyzed fluorimetrically, blank protease solu-

TABLE I. **Calibration of the spectrofluorimeter with spectral profiles.**

Sample	State of derivatization	A (nm)	O (nm)	B (nm)
BSA	0	–	341.4	–
	1	320.6	341.8	366.6
	2	321.4	–	364.8
Lysozyme	0	–	339.6	–
	1	316.4	342.0	376.0
	2	316.0	–	372.0
Lysozyme (4M urea)	0	–	338.8	–
	1	316.0	340.0	364.4
	2	316.2	–	364.2

Position in emission spectra having maximum positive gradient (A); zero gradient, *i.e.* λ_{max}, em. (O); maximum negative gradient (B). - indicates determination was not possible.

tions serving as controls.

Other Methods—All samples were centrifuged and passed through Spartan 3 Nylon filters (pore size, 0.45 mμ; Schleicher & Schull) to remove particulate matter, although scattering does not interfere with fluorescence emission to any significant extent (*1*). Dispensing of liquids was performed with a Hamilton syringe (Australia), the precision being ± 2%.

RESULTS

Characters of the Second Derivative Spectra of NATA—Analysis of the second derivative emission spectra of NATA, with excitation at 295 nm, was performed because of its structural similarity with tryptophans as they occur in proteins. NATA (10 nM) in 20 mM K-phosphate buffer, pH 7.5, shows emission effectively between 303–450 nm, em_{max} being 338.5 ± 0.6 nm. The second derivative spectrum showed two distinct troughs in the negative ordinate, at 340 ± 1.0 nm (A) and 358.5 ± 1.0 nm (B), the former being of higher intensity (Fig. 1). The ratio of the intensities at B and A as measured from zero ordinate to the trough valley has been termed R, and was found to be 0.70 ± 0.05. 10 nM tryptophan in the same buffer yields a similar second derivative spectrum. For tryptophan analogues and proteins, the changes of spectral patterns with different solvent compositions were most prominent in the negative ordinate (discussed later). The positive ordinate was apparently featureless and is not considered here.

The intensities at A and B were found to be linearly dependent on the concentration of NATA in the range of 0–30 nM. Moreover, R as well as the spectral positions of both A and B were found to be invariable. Higher concentrations of NATA could not be checked because the spectrofluorimeter readings were less accurate at that stage. R, being independent of the fluorophore concentration, is free from dispensing error too. The two troughs observed might be the characters of a chemically and environmentally homogeneous fluorophore or may originate from a heterogeneous population of fluorophores of a similar chemical nature. To distinguish this, the excitation wavelength for NATA (10 nM) was varied between 280–300 nm, where most of the aromatic residues exhibit absorption maxima. The intensities at A and B varied depending on the wavelength of excitation but R was found to be invariable within the limits of error (0.70 ± 0.05). The results are presented in Fig. 2. Variation of the temperature (15–70°C), pH (4–10), and ionic strength (0–2 M NaCl) had no effect on R. Under various conditions in aqueous buffer, NATA produced superimposable underivatised emission spectra after normalization, although minor or insignificant differences were evident at the emerging and trailing ends of the spectra. Variability of spectral data to that extent could not change R, indicating the reliability of this index (Fig. 2).

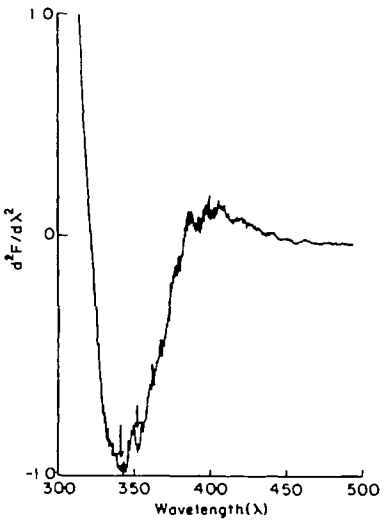

Fig. 1. **Second derivative fluorescence emission spectra of 10 nM NATA.** Excitation was performed at 295 nm and emission was followed between 300–500 nm in 20 mM potassium-phosphate buffer, pH 7.5. $d^2F/d\lambda^2$ indicates derivative intensity. The two arrows indicate spectral troughs at wavelengths of 338.5 nm (A) and 358.5 nm (B).

Wavelength dependence of monochromator transmission efficiency, which is a limitation for some spectrofluorimeters, results in anomalous shoulders in the emission spectrum. This could then appear as troughs and extrema in first and second derivative spectra. The emission spectrum of *N*-acetyl tyrosine after excitation at 280 nm shows an em_{max} at 321.2 nm and is well extended up to 360 nm in aqueous buffer at pH 7.0. Under various conditions, *e.g.* variation of the excitation wavelength between 260–280 nm, concentration of the fluorophore between 0–100 nM, and ionic strength of the buffer between 0–1 M, second derivative spectra were generated. These derivative spectra were distinctly different from that of NATA, indicating that the data reported for NATA, *e.g.* existence of two troughs at the negative ordinate, are not associated with any instrumental artifact. The success of the experiment is due to the quality (smoothness) of the zero-order emission spectra generated with an instrument. On the other hand, when B does not appear as a distinct peak, for example, where R appears to be lower than 0.1, uncertainty arises as to proper assignment of the numerical value of B. In such cases, repeated scans were performed and derivative values at 358.5 nm were considered.

Effects of Tyrosine and Quenchers—Tyrosine exhibits very low but finite absorption at 295 nm. With excitation at that wavelength, *N*-acetyl tyrosine (10 mM) in 20 mM K-phosphate buffer, pH 7.5, does not show any significant emission and hence no derivative intensity between 315–500 nm (Fig. 3). Variation of the molar concentration of *N*-acetyl tyrosine up to a 40-fold molar excess over 10 nM NATA failed to change R (Fig. 3, inset). Quenchers like acrylamide (0–0.8 M), potassium iodide (0–0.4 M), and trichloroethanol (0–0.4 M) were included separately with 10 nM NATA. The quenchers decreased the emission intensities in a concentration-dependent manner without altering the emission maxima. Derivatization of the quenched spectrum showed gradual decreases of the intensities at A and B, but R was found to be invariable.

Effect of Solvent Polarity—It is well known that tryptophan fluorescence is dependent on solvent polarity (*19, 20, 23*). Variation of the solvent dielectric constant (DEC) from 78 to 2.21 at 25°C, using various organic solvents in place of aqueous buffer, showed that the height of the trough at B relative to A decreased, and as a result R changed from 0.70 ± 0.05 to 0.07 ± 0.05. This was accompanied by a 2–5 nm blue shift of the positions of A and B. Nor-

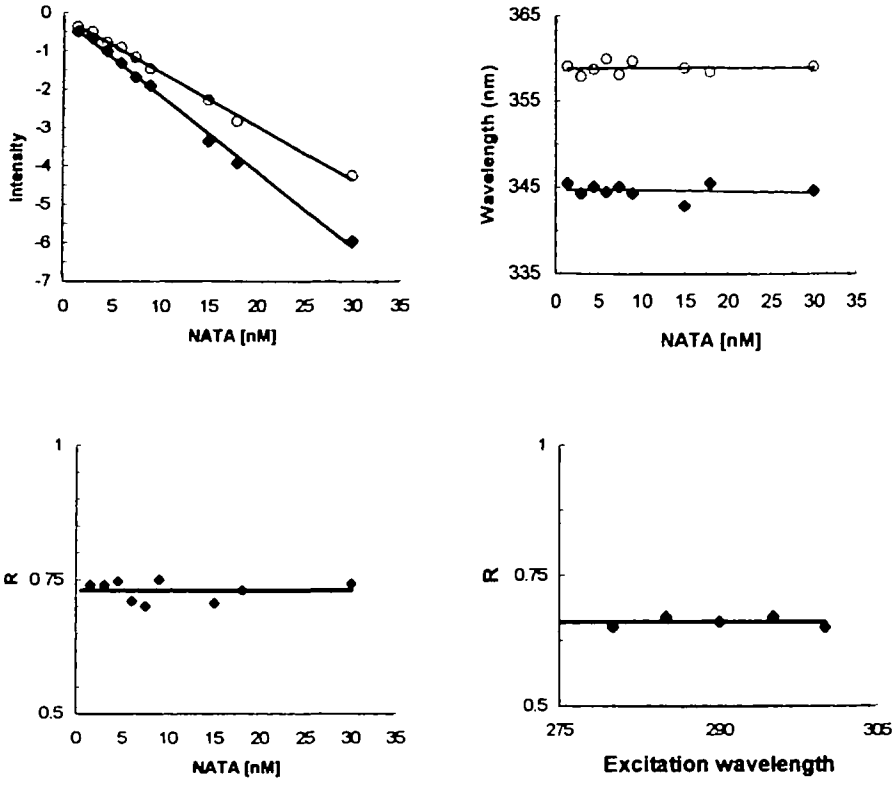

Fig. 2. **Dependence of derivative characters of NATA on external conditions.** (Upper left) Derivative intensities of 0–30 nM NATA at 338.5 nm (A) (◆) and 358.5 nm (B) (○). (Upper right) Wavelength of the trough position at (A) (●) and (B) (○) in Fig. 1 on variation of the concentration of NATA. (Lower left) R, ratio of derivative values of B *versus* A with the concentration of NATA, and (lower right) R with the excitation wavelength between 280–300 nm. The excitation and emission band passes were 10 nm each, as compared to 5 nm in Fig. 1, resulting in higher derivative intensities at A and B, but the spectral characters remained unaltered.

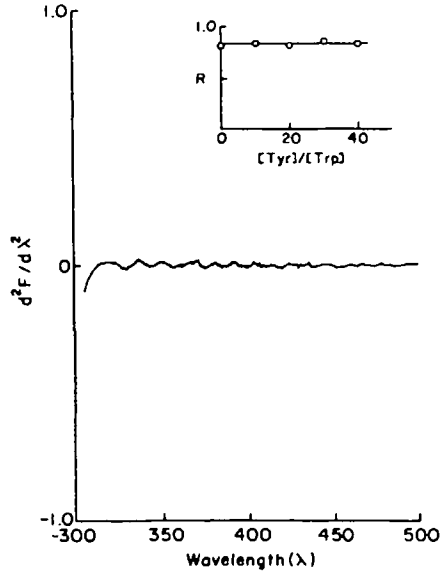

Fig. 3. **Derivative spectrum of *N*-acetyl tyrosine (10 nM) at pH 7.5 after excitation at 295 nm.** (Inset) Dependence of R (as described in the text) on 10 nM NATA in presence of a 0–40 fold molar excess of *N*-acetyl tyrosine. $d^2F/d\lambda^2$ indicates derivative intensity.

malized second derivative spectra of NATA in low ionic strength aqueous buffer, methanol, ethanol and acetonitrile are presented in Fig. 4A, illustrating the change of spectral characters. The dependence of R on solvent DEC ranging from 78.54 to 2.21 exhibited a linear relation with a regression coefficient of 0.961 (Fig. 4B).

Theoretical considerations have indicated that differences in dielectric constant might be the major but not the only criteria responsible for the changes of the emission spectra of a fluorophore in different solvents (*19, 20*). The chemical structures of the solvent and solute, for example, polar and non-polar segments, also play roles in stabilizing Frank-Cordon states (*23, 24*). This factor could largely be removed by using two solvent systems, like water-methanol, *etc.*, while preparing solvents of predetermined DEC (*25*). The relation of R to increasing concentrations of methanol, ethanol and acetonitrile in water was followed in detail (Fig. 5). In all cases, linear negative dependency of R with increasing organic solvent concentration was observed, the regression coefficients being 0.994, 0.993, and 0.992, respectively. The better fit of linearity in Fig. 5, as compared to in Fig. 4B, possibly arises from the spectral quality of the three solvents as well as the advantage of a two-solvent system stated above. Among all the solvents tested so far only acetonitrile yields relatively low R compared to its DEC. The reason for this has not been investigated yet.

Second Derivative Spectra of Proteins—Ten well characterized proteins, *e.g.* ribonuclease, peroxidase, ovalbumin, pyruvate kinase, hexokinase, epimerase (*E. coli*), lysozyme, phospholipase C, galactose-1-phosphate uridyl transferase, galactose oxidase, and BSA, were studied. Their concentrations were kept between 0.5–1.0 μM in 20 mM K-phosphate buffer, pH 7.5. With excitation at 295 nm, the derivatised emission spectra were found to be similar to that of NATA in solvents of considerably low polarity. Two troughs in the negative ordinate were apparent at 340 ± 2.0 and 358.5 ± 2.0 nm, the former being prominent. R varied between 0.02–0.34. In cases where the value was less

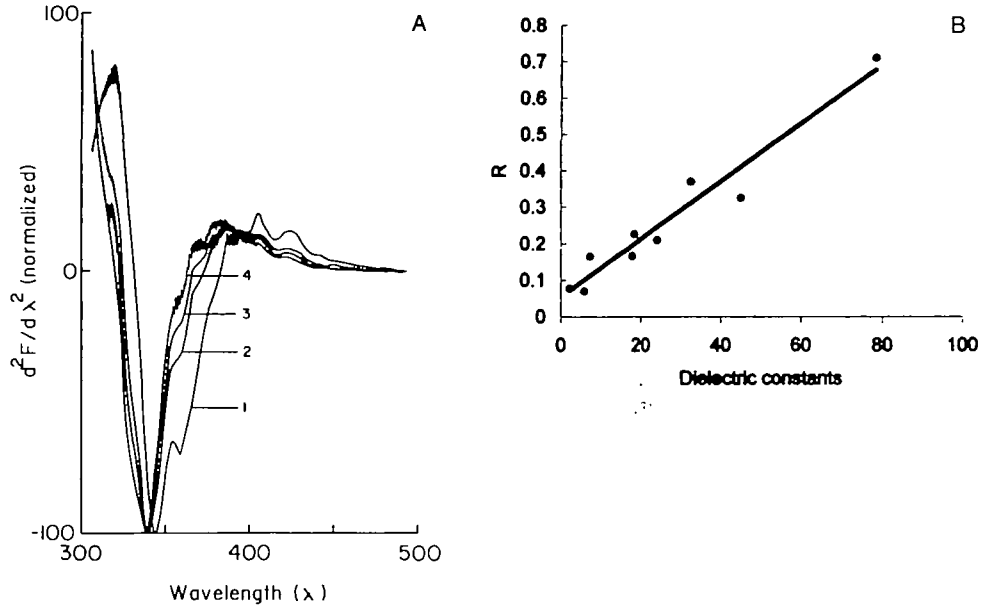

Fig. 4. **Dependence of R of NATA on solvent dielectric constants.** (A) Normalized derivative spectra of NATA in the presence of water (1); methanol (2); ethanol (3); and acetonitrile (4). (B) Linear dependency of R on the solvent dielectric constants. The solvents used were as follows (DEC in parenthesis): 1,4-dioxane (2.21); ethyl acetate (6.0); tetrahydrofuran (7.4); 1-butanol (17.8); 2-propanol (18.3); ethanol (24.3); methanol (32.63); dimethyl sulphoxide (*45*); and water/aqueous buffer (78.54). The regression coefficient was 0.961. The original stock of NATA was maintained in dehydrated ethanol.

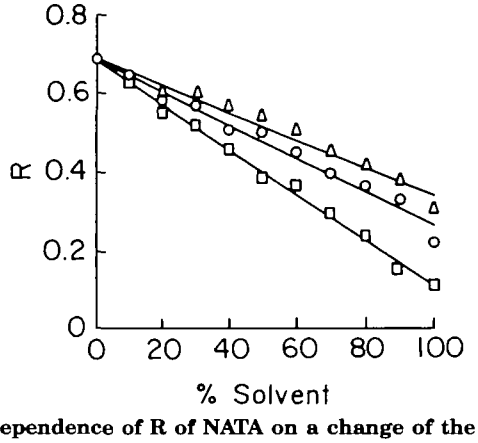

Fig. 5. **Dependence of R of NATA on a change of the solvent composition from aqueous to organic.** The solvents used were methanol (△); ethanol (○), and acetonitrile (□).

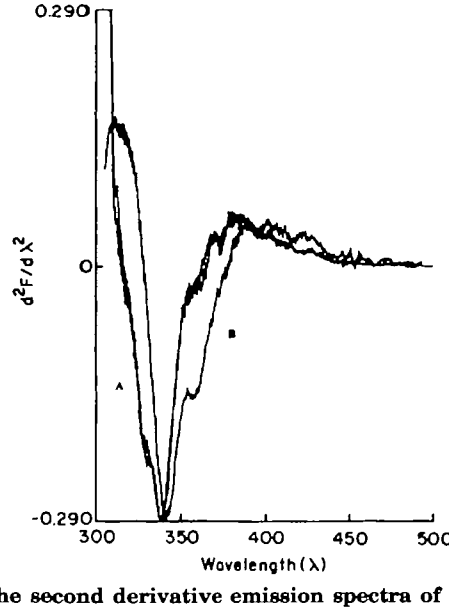

Fig. 6. **The second derivative emission spectra of native (A) and unfolded (B) epimerase between 300–500 nm after excitation at 295 nm.** The refolded protein has spectra overlapping those of the native conformer. The protein concentration was 40 μg/ml.

than 0.05, there was some uncertainty as to its evaluation because of the not so smooth nature of the derivative profiles. The derivative values at 358.0 nm were considered to deduce R after repeated scans. Low values of R illustrate the general buried nature of tryptophan residues of proteins in a hydrophobic environment (*19, 26, 27*). A representative picture with epimerase is presented in Fig. 6 (tracing A). Although not concerned in the present study, derivative spectra of proteins, unlike NATA, sometimes show a shoulder or notch to the left of A. The discrepancy possibly arises from the presence of stable and complex tertiary structures of proteins leading to different arrays of energy states. The manifestation might be insignificant in zero-order emission spectra but is amplified after derivatization.

All proteins mentioned earlier yielded R between 0.003–0.005 in the presence of 0.1% SDS in the phosphate buffer. This is consistent with the fact that SDS forms a very strong hydrophobic layer on a protein surface inducing denaturation (*28*). Unfolding of proteins in the presence of strong denaturants like 8 M urea or 6 M Gdm, HCl led to destabilization of the structure, whereby buried tryptophan residues are exposed to aqueous solvents (*29, 30*). To check whether this is reflected in the derivative spectrum, four proteins with or without cysteine bridges, *e.g.* BSA, lysozyme, ovalbumin and epimerase, were selected. The unfolding buffer was supplemented with 2-MCE to reduce disulphide bonds. An increase of R compared with in the native state was evident, 0.222–0.572 with urea and 0.458–0.622 with Gdm, HCl/2-MCE. The unfolded states sometimes withstand a strong hydrophobic core that acts as a nucleation site during refolding (*30*). This might prevent the

unfolded protein from attaining the R value reached by NATA in aqueous buffer. Eight of the above ten proteins were also extensively proteolysed with trypsin and chymotrypsin, with the aim to generate small unstructured peptides, where tryptophan residues were expected to be solvated. R of the proteolysed products varied between 0.60–0.93. Why the higher limit exceeded that of NATA, *i.e.* whether or not this originates from the effects of neighboring amino acids of small peptides is not clear. As an alternate consideration, six of the previously unfolded proteins were refolded by dilution with buffer. R of the refolded states varied between 0.066–0.48, suggesting an approach to their native conformations. In the case of epimerase, normalized derivative spectra of the native and refolded states show indistinguishable profiles, which were distinctly different from that of the unfolded state (Fig. 6, tracing A *versus* B). This illustrates that in the case of epimerase, environment of the tryptophan residues of the refolded state largely resembles that of the native state. For other proteins, deviation of R from that of the native state most probably arose from incomplete or improper recovery of the structure of the refolded state (*31, 32*). The results of the protein unfolding-folding studies are summarized in Table II.

Furthermore, it was examined whether or not R could be used as a parameter to follow the unfolding transitions of proteins with denaturants like 0–8/10 M urea and 0–6/8 M Gdm, HCl in the presence or absence of a reducing agent to break disulphide linkages. Four systems were selected: (a) chicken egg white lysozyme (50 μg/ml) (14.3 kDa with 4 cystine bridges) was treated with 0–8 M Gdm, HCl in the presence of 10 mM 2-MCE at 30°C for 16 h to generate partial and total equilibrium unfolded states. For each set, the same solvent was incubated similarly as a control. The derived R was 0.221–0.222 and 0.666–0.667 between 0–2 M and 4–8 M Gdm, HCl, respectively. This was associated with a cooperative transition having a midpoint at approximately 3.0 M Gdm, HCl. The derivative profiles of the pre- and post-transition zones are shown in Fig. 7A. The latter clearly shows a significant change of the derivative intensity at B. The position of A in the post-transition profiles exhibited a red shift of about 5 nm, which was similar to that of NATA, with a change from lower to higher solvent dielectric constants. The transition profile is shown in Fig. 7B (upper tracing). This may be compared with the sharp cooperative transition of the same protein under identical conditions observed from optical rotatory dispersion at 234 nm (*33, 34*). The mid-point of the ORD experiment was around 3.6 M. While ORD data represent the secondary structures of a protein, R is associated with the tertiary

TABLE II. **Proteins and their R values in the native, proteolysed, denatured, and refolded states.**

Protein	PDB Code[a]	Native state	Proteolysed state	In 8 M Urea/6 M Gdm, HCl + 10 mM MCE	Refolded state
BSA	–	0.24	0.69	0.47/0.62	0.15
Lysozyme	6 LYT	0.19	0.75	0.22/0.59	0.17
Ovalbumin	1 OVA	0.05	0.62	0.57/0.62	0.07
UDP-galactose 4-epimerase	2 UDP	0.066	0.60	0.355/0.46	0.072
Peroxidase	3 ATJ	0.07	0.93	N.D.[b]	N.D.
Hexokinase	1 GLK	0.16	0.64	N.D.	0.21
Phospholipase C	1 AH7	0.34	0.89	N.D.	N.D.
Galactose 1-phosphate uridyl transferase	1 GUP	0.11	0.65	N.D.	N.D.
Pyruvate kinase	1 PKN	0.095	N.D.	N.D.	N.D.
Ribonuclease T1	1 BVI	0.15	N.D.	N.D.	N.D.
Galactose oxidase	1 GOF	0.025	N.D.	N.D.	N.D.

[a]Protein data bank. [b]N.D., not determined.

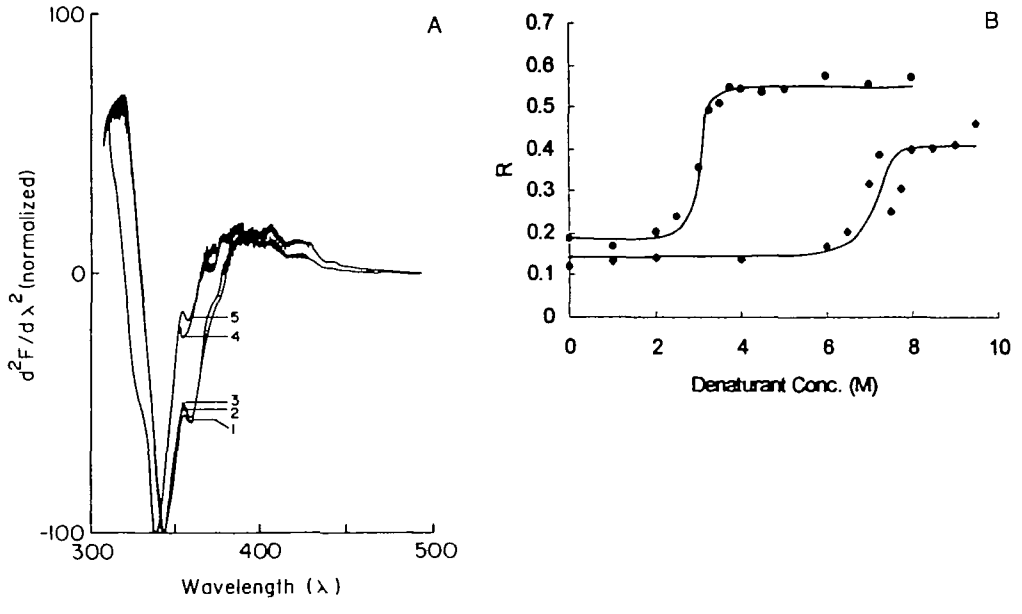

Fig. 7. **Derivative profiles of equilibrium unfolding intermediates of proteins.** (A) Normalized derivative spectra of lysozyme in 50 mM sodium phosphate buffer, pH 7.5, in presence of (1) 8 M; (2) 6 M; (3) 4 M; (4) 2 M; and (5) 0 M Gdm, HCl containing 10 mM 2-MCE. These spectra essentially represent post- and pre-transition zones. Other spectra have not been included to ensure clarity. (B) Unfolding transition profiles of lysozyme by Gdm, HCl in the presence of 2-MCE (●), and liver alcohol dehydrogenase in the presence of urea (◆) as monitored against R.

structure, which is more sensitive to solvent perturbation resulting in a minor difference in the two transition midpoints. When the same transition was followed with 0–10 M urea in the absence of 2-MCE, R remained almost unchanged between 0.222–0.225, indicating the stability of the native structure due to the disulphide bridges. (b) Equilibrium unfolded states of liver alcohol dehydrogenase (LAD) (0.25 mg/ml), a tetrameric molecule devoid of disulphide bridges, were generated with 0–10 M urea at 30°C for 16 h. The unfolding, as observed as R, showed a transition essentially between 7–8 M urea, the mid-point being 7.2 M (Fig. 7B, lower tracing). Such stability of the molecule against denaturation, dissociation of subunits and change of the tertiary structure have also been reported earlier, for example, between 7–8 M urea or 5–6 M Gdm, HCl with fluorescence polarization (*35, 36*). (c) Similarly, the transition midpoint of BSA with 0–8 M urea was found to be at around 6.0 M (result not shown) (*37*). This is comparable to 5.8 M observed on 0–8 M urea gradient transverse polyacrylamide gel electrophoresis (*38*), and finally (d) unfolding transitions of epimerase with R between 0–8 M urea showed unfolding was essentially complete with 6 M urea, a similar conclusion being arrived at on circular dichroism spectroscopy. The transition midpoint at 3.1 M urea was very close to 3.0 M derived from fluorescence emission spectra (ex: 295 nm; em: 335 nm) of the unfolding intermediates, which was associated with both quenching and red shift of emission. The details of the results have been communicated elsewhere (*37, 39*). Thus R could faithfully represent the unfolding transitions of proteins, which are supported by other physical techniques.

DISCUSSION

The second derivative emission spectra of NATA, presented in Fig. 1, are similar but not identical to as previously reported (*9*). Earlier, a Perkin–Elmer instrument (Model MPF-44B) equipped with a differential corrected spectra unit, Hitachi Perkin–Elmer DSCU-2, inserted between the signal output and the recorder output was used. That system apparently failed to resolve troughs in the negative ordinate of the spectrum, which is at present possible with instruments of later versions. An index, R, based on the intensities at the two trough positions was found to be related with the hydrophobicity of the medium. For an underivatized spectrum of NATA, a change of the solvent from 1,4-dioxane (DEC = 2.21) to aqueous buffer (DEC = 78) is associated with a shift of em_{max} from 335.0 → 350.0 nm. In comparison to 1–2 nm variation in recording em_{max}, this parameter is not too sensitive to the solvent polarity. However, a corresponding change of emission intensity from 184 to 71 (arbitrary units) provides sufficiently accurate a parameter for monitoring, the numerical difference being large. Therefore, for NATA, derivatization *per se* does not have any additional advantage. However, the results presented here indicate that R is independent of the presence of tyrosine and quenchers, and also remains invariant with changes of the concentration of the fluorophore, pH, temperature, ionic strength of the buffer, wavelength of excitation, *etc.* in the range of biological significance (Figs. 2 and 3, also see the text). With this background, the observation was extrapolated to proteins.

It is worthwhile to consider how similar the tryptophan emission spectra of proteins are to that of NATA in aqueous buffers to justify comparisons. Two differences are obvious; tryptophans in proteins are largely in a hydrophobic environment causing spectral shifts, and secondly protein emissions are polarized due to rotational restrictions arising from far heavier molecular weights than that of NATA. In addition to a general wavelength response, emission monochromators sometimes exhibit a bias for one plane of polarization over the other, and this bias is wavelength-dependent. Furthermore, in addition to a gradual change in this bias with wavelength, there are several wavelengths where the so-called "Woods anomaly" occurs (*40*). At that point one will observe dramatic bumps in the "corrected" emission spectrum, which is due to the fact that at the Wood's anomaly wavelength, all perpendicularly polarized components are lost. Whether such a discrepancy occurs in the protein emission leading to notches in the derivative spectrum requires verification.

Experiments with NATA were performed to generate three sets of emission spectra (ex: 295 nm); one without any polarizer at excitation and emission windows as a control, and two others having no polarizer at the excitation window but with one at either 0° and 90°, respectively, at the emission window. The intensity of emission of these spectra differed as expected because of the change of emission windows, but when normalized they were nearly overlapping. em_{max} for these sets were 353.4, 356.0, and 355.4 nm, respectively. Moreover, in none of these spectra was a notch, hump or shoulder observed, indicating that the emission monochromator does not show any wavelength-dependent response for either perpendicularly or horizontally polarized light (result not shown). Identical experiments were performed with BSA. Three sets of emission spectra, together with one for NATA without any polarizer as a reference, were normalized (Fig. 8). The BSA emissions were not identical, possibly suggestive of wavelength-dependence of emission monochromators, but the differences were not significant in terms of normal variation of spectral parameters, for example em_{max} of these spectra were 343.8, 344.8, and 344.2 nm, respectively. Similar results showing variation of spectral data were observed with lysozyme (338.6, 340.0, and 340.2 nm) and ovalbumin (336.0, 339.0, and 338.0 nm). Therefore a minor qualitative difference between the derivative spectra of NATA and a protein is expected. But in all cases the polarized emission

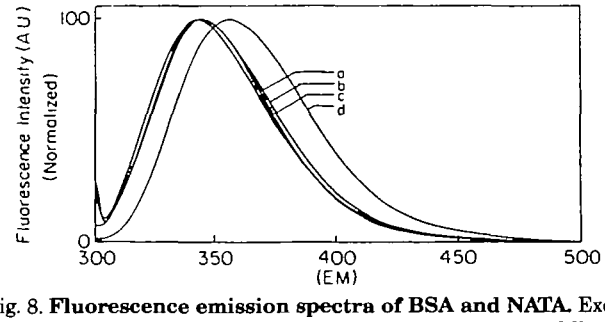

Fig. 8. **Fluorescence emission spectra of BSA and NATA.** Excitation was performed at 295 nm. The tracings were as follows: NATA (unpolarized) (a); BSA (unpolarized) (b); BSA (polarizer at 0° only at the emission window) (c); and BSA (polarizer at 90° only at the emission window) (d). Emission intensities were normalized at the respective emission maxima.

spectra were smooth and free from any notch, asymmetry or hump. The derivative spectra of these polarized emission, except for a minor shift of trough positions (±2 nm), also did not demonstrate any unusual peak, trough, notch, or hump other than as observed in the cases of unpolarized emission (Fig. 3). These findings indicate the absence of Wood's anomaly, at least in the wavelength zone studied.

In an ideal situation, all spectrofluorimeters should yield identical spectra for a protein provided proper solvent corrections including instrumental calibrations, if any, have been performed. In reality the emission spectra of proteins sometimes differ depending on the instrument, which in turn is related to the wavelength dependence of emission monochromators. Thus, the characters of the derivative spectra also change. To check this, different spectrofluorimeters available in our locality were used, as follows: Hitachi F 4020 (this institute), Hitachi F 4020 (Department of Life Science, Jadavpur University, Calcutta), Hitachi F 4020 (Biochemistry Department, University of Calcutta), and Hitachi F 4500 (this institute). While most of the experiments presented here were performed with the Hitachi F 4020 of our institute, overlapping data were found when some of the experiments described in Figs. 1–4 were performed with the same instrument of Jadavpur University. Derivative spectra of NATA and BSA (native and denatured states) were also generated with all other instruments. No significant difference leading to anomalies was detected. Thus the observations presented here are not dependent on the instrument make or model.

For proteins, exposure of tryptophans from the interior hydrophobic environment to aqueous media, *e.g.* during unfolding or extensive proteolysis, is usually associated with changes of emission maxima. The numerical difference is often smaller than in the case of NATA. On the other hand, due to quenching effects of neighboring amino acids, unfolding or other change of conformations might be associated with enhancement, quenching or non-alteration of emission intensity (*41*). This may be compared with the large difference in R during such processes, say from 0.07 to 0.70. Thus, derivatization offers a more reliable and sensitive spectral parameter for following the tryptophan environments of protein molecules.

In an attempt to correlate the average hydrophobicity of tryptophan residues of proteins listed in Table II with derived R, their X-ray crystallographic structures were analyzed. The structures were downloaded from a Protein Data Bank file using the four letter codes, as mentioned in Table II. The average hydrophobocity of tryptophan residues of a protein was calculated as follows: using an Insight-11 software program with each tryptophan residue as the center, cubes of different arm length were constructed. All the amino acids within these cubes were listed and their hydrophobicity was taken from the index provided in (*42*). In cases where a tryptophan residue was not completely surrounded by other amino acids, *i.e.* had contact with the solvent, the respective surface accessibility (a numerical fraction) was obtained with the same software program. The arithmetic mean of the hydrophobocity of all amino acids in a cube multiplied by the fraction buried (1–surface accessibility) was considered as the contribution of a particular tryptophan residue towards the hydrophobicity of a protein. For multitryptophan proteins, further averaging of the hydrophobicity of tryptophans was performed for final evaluation. The whole procedures were repeated for cubes of arm lengths 2.5, 3, 3.5, and 4 Å since interaction of an amino acid at a distance more than 4 Å becomes insignificant (*43*). Unfortunately no correlation between hydrophobicity, as derived with different cube lengths, and R was apparent for the proteins mentioned here.

It is thus apparent that although parameter "R" senses major conformational changes of proteins, its accurate correlation with the native state is not possible at this moment. There seem to be three reasons. The method adopted for determination of hydrophobicity of proteins may need further refinement. Experimental determination of R for proteins in the native state is usually inaccurate as the intensity of the trough at 358.5 nm is very low and the fluorescence emission patterns of proteins may be associated with such phenomena as 'charge transfer complex,' *etc.* making the derivative spectrum dissimilar to that of NATA (*19, 20, 44*). Further studies may resolve these shortcomings.

Prof. R. Doolittle, University of California at San Diego, and Dr. Samrajnee Dutta, Chemistry Department, Presidency College, Calcutta, helped in the crystallographic analysis. We also thank an anonymous reviewer for pointing out the polarization effect of protein fluorescence emission in the consideration of a derivative spectrum.

REFERENCES

1. Butler, W.L. (1979) Fourth derivative spectra. *Methods Enzymol.* **56**, 501–515
2. Mach, H., Thomson, J.A., Midaugh, C.R., and Lewia, R.V. (1991) Examination of phenylalanine micro-environments in proteins by second derivative absorption spectroscopy. *Arch. Biochem. Biophys.* **287**, 33–40
3. Mach, H., Dong, Z., Midaugh, C.R., and Lewia, R.V. (1991) Conformational stability of Cu,Zn-superoxide dismutase, the apoprotein and its Zn substituted derivatives; second derivative spectroscopy of phenylalanine and tyrosine residues. *Arch. Biochem. Biophys.* **287**, 41–47
4. Havel, H.A., Kauffman, E.W., Plaisted, S.M., and Brens, D.N. (1986) Reversible self-association of bovine growth hormone during equilibrium unfolding. *Biochemistry* **25**, 6533–6538
5. Bewley, T.A. and Li, C.H. (1984) Conformational comparison of human pituitary growth hormone and human somatotropin (human placental lactogen) by second order absorption spectroscopy. *Arch. Biochem. Biophys.* **233**, 219–227
6. Bewley, T.A. and Li, C.H. (1986) The conformation of monkey pituitary somatotropin. *Arch. Biochem. Biophys.* **248**, 646–651
7. Havel, H.A. (1996) *Spectroscopic Methods for Determining Protein Structure in Solution*, pp. 62–68, VCH Publishers, New York
8. Ragone, R., Colonna, Servillo, G., and Irace, I.G. (1985) Resolution of overlapping bands in the near UV absorption spectrum of indole derivatives. *Photochem. Photobiol.* **42**, 505–508
9. Garcia-Borron, J.C., Escribano, J., Jimenez, M., and Iborra, J.L. (1982) Quantitative determination of tryptophanyl and tyrosyl residues of proteins by second-derivative fluorescence spectroscopy. *Anal. Biochem.* **125**, 277–285
10. Singh, R., Suri, R., and Agarwal, C.G. (1995) Flourescence properties of oxidised human plasma low-density lipoproteins. *Biochim. Biophys. Acta* **1254**, 135–139
11. Mahedero, M. C., Salinas, F., and Aaron, J.J. (1994) Determination of sulphanilamide in milk by first-derivative and second-derivative spectrofluorimetry. *J. Pharm. Biomed. Anal.* **12**, 1097–1101
12. Damiani, P., Ibanez, G., and Olivieri. A.C. (1994) Zero-crossing first and second derivative synchronous fluorescence spectroscopic determination of aspirine metabolites in urine. *J. Pharm.*

Biomed. Anal. **12**, 1333–1335
13. Torrado, S. and Cadorniga, R. (1994) Comparison of assay methods by second-derivative spectroscopy, colorimetry and fluorescence spectroscopy of salisylic acid in aspirine preparation with a high performance liquid method. *J. Pharm. Biomed. Anal.* **12**, 383–387
14. Fox, T., Ferreira–Rajabi, L., Hill, B.C., and English, A.M. (1993) Quenching of intrinsic fluorescence of yeast cytochrome *c* peroxidase by covalently and non-covalently bound quenchers. *Biochemistry* **32**, 6938–6943
15. Saha, A., Mandal, P.C., and Bhattacharyya, S.N. (1993) Tyrosine residues in unirradiated and gamma-irradiated dihydroorotate dehydrogenase: fluorimetric and second-derivative absorption spectrophotometric studies. *Int J. Radiat. Biol.* **63**, 557–564
16. Wilson, D.B. and Hogness, D.S. (1969) The enzymes of galactose operon in *Escheriachia coli*. II. The subunits of uridine diphosphogalactose 4-epimerase. *J. Biol. Chem.* **244**, 2132–2136
17. *Handbook of Biochemistry and Molecular Biology* (1970) pp. C71–C98, 2nd ed., CRC Press, Cleveland
18. Lowry, O.H., Rosenbrough, N.J., Farr, A.L., and Randall, R.J. (1951) Protein measurement with the folin-phenol reagent. *J. Biol. Chem.* **193**, 265–276
19. Lakowich, J.R. (1982) *Principles of Fluorescence Spectroscopy*, pp. 187–215, Plenum Press, New York & London
20. Bradn, L. and Witholt, B. (1967) Fluorescence measurements. *Methods Enzymol.* **11**, 776–856
21. Roder, H. and Elove, G. (1993) Early stages of protein folding in *Mechanisms of Protein Folding* (Pain, R.H., ed.) pp. 26–54, Oxford University Press, London
22. Ptitsyn, O.B. (1995) Molten globule and protein folding. *Adv. Protein Chem.* **47**, 83–229
23. Pease, A.J., Rosen, C.-G., and Pasby, T.L. (1971) *Fluorescence Spectroscopy: An Introduction to Biology and Medicine*, pp. 65–86, Marcel Dekker, New York
24. Glasstone, S. and Lewis, D. (1961) *Elements of Physical Chemistry*, pp. 265–277, MacMillan, London
25. Haque, Md. E., Ray, S., and Chakrabarti, A. (2000) Polarity estimate of the hydrophobic binding sites in erythroid spectrin: A study by pyrene fluorophore. *J. Fluors.* **10**, 1–6
26. Roder, H., Elove, G.A., and Englander, S.W. (1988) Structural characterization of folding intermediates in cytochrome c by H-exchange labelling and proton NMR. *Nature* **335**, 700–705
27. Fauchere, J.L. (1985) How hydrophobic is tryptophan? *Trends Biochem. Sci.* **10**, 268
28. Weber, K. and Osborn, M. (1975) Proteins and sodium dodecyl sulfate: molecular weight determination on polyacrylamide gels and related procedures in *The Proteins* 1, 3rd ed., pp. 179–223, (Neurath, H. and Hill, L.R., eds.) Academic Press, New York,
29. Pace, C.N. and Scoltz, J.M. (1997) Measuring the conformational stability of proteins in *Protein Structure, A Practical Approach*, 2nd ed. (Creighton, T.E., ed.) pp. 299–322, IRL Press, Oxford
30. Richard, F.M. (1992) Folded and unfolded proteins: an introduction in *Protein Folding* (Creighton, T.E., ed.) pp. 1–58, Freeman W.H. and Company, New York
31. Dutta, S., Maity, N.R., and Bhattacharyya, D. (1997) Reversible folding of UDP-galactose 4-epimerase from *Escherichia coli*. *Eur. J. Biochem.* **244**, 407–413
32. Fischer, G. and Schmid, F.X. (1990) The mechanism of protein folding: implications of *in vitro* refolding models for *de novo* protein folding and translocation in the cell. *Biochemistry* **29**, 2205–2212
33. Tanford, C. (1968) Protein denaturation. *Adv. Protein Chem.* **23**, 121–282
34. Tanford, C., Pain, R.H., and Otchin, N.S. (1966) Equilibrium and kinetics of the unfolding of lysozyme (muramidase) by guanidine hydrochloride. *J. Mol. Biol.* **15**, 489–504
35. Branden, C-I., Jornvall, H., Eklund, H., and Furugren, B. (1975) Alcohol dehydrogenase in *The Enzymes* (Vol. XI, Part A Boyer, P.D., ed.) 3rd ed., pp. 103–190, Academic Press, New York
36. Green, R.W. and McKay, R.H. (1969) The behavior of horse liver alcohol dehydrogenase in guanidine hydrochloride solution. *J. Biol. Chem.* **244**, 5034–5043
37. Nayar, S. (2000) Studies on the subunit structure and folding behavior of a complex multimeric protein: UDP-galactose 4-epimerase. Ph.D. Thesis, Jadavpur University, Calcutta, India
38. Creighton, T.E. (1979) Electrophoretic analysis of the unfolding of proteins by urea. *J. Mol. Biol.* **129**, 235–264
39. Nayar, S. and Bhattacharyya, D. (2001) UDP-galactose 4-epimerase from *Escherichia coli*: Equilibrium unfolding studies. *Indian J. Biochem. Biophys.* **38**, 353–360
40. Mac Donald M.E., Alexanian, A., York, R A., Popovic, Z., and Grossman, E.N. (2000) Spectral transmittance of Lossy printed resonant grid Terahertz bandpass filters *Trans. Microwave Theory Tech.* **48**, 712–718
41. Eftink, M.R. and Shastri, M.C.R. (1997) Fluorescence methods for studying kinetics of protein-folding reactions. *Methods Enzymol.* **278**, 258–286
42. Kyte, J. and Doolittle, R.F. (1982) A simple method for displaying the hydropathic character of a protein. *J Mol Biol.* **157**, 105–132
43. Chothia, C. (1984) Principles that determines the structure of proteins. *Ann. Rev. Biochem.* **53**, 537–571
44. Donovan, J.W. (1973) Ultraviolet difference spectroscopy—New techniques and applications. *Methods Enzymol.* **27**, 497–525.